

# Tanshinone IIA Promoted Autophagy and Inhibited Inflammation to Alleviate Podocyte Injury in Diabetic Nephropathy

Yuan Li<sup>1</sup> , Tong Wu<sup>1</sup>, Hongye Li<sup>2</sup>, Mingming Liu<sup>2</sup>, Haiyan Xu<sup>1</sup>

<sup>1</sup>School of Basic Medicine, Xuzhou Medical University, Xuzhou, 221004, People's Republic of China; <sup>2</sup>Lianyungang Clinical School of Xuzhou Medical University, Lianyungang, 222006, People's Republic of China

Correspondence: Haiyan Xu, School of Basic Medicine, Xuzhou Medical University, Xuzhou, 221004, People's Republic of China, Email xhy\_8@163.com

**Purpose:** Tanshinone IIA (Tan-IIA) is widely used in patients with diabetic nephropathy (DN), but its protective effect on podocytes in DN has not been well studied. In this study, the effects of Tan-IIA on autophagy and inflammation of glomerular podocytes in DN were observed in vivo and in vitro, and the underlying mechanisms were investigated. Irbesartan, an angiotensin II receptor blocker, is a representative medication for the clinical treatment of DN. So irbesartan was chosen as a positive control drug.

**Methods:** Eight-week-old male db/db mice were randomly divided into a DN group, an irbesartan group, and three groups receiving different doses of Tan-IIA. The control group consisted of the db/m littermate mice. Blood, urine, and kidney samples were taken from the mice after 12 weeks of continuous administration. Renal protection of Tan-IIA was evaluated using enzyme-linked immunosorbent assay kits, haematoxylin and eosin staining, transmission electron microscopy, Western blotting, and immunohistochemistry. In vitro, the protective effect of Tan-IIA on podocytes was explored using MPC5 cells cultured with high glucose.

**Results:** Tan-IIA significantly improved renal pathological injury and relieved the renal dysfunction in DN. Compared with the DN group, Tan-IIA could up-regulate the expression of Synaptopodin, Podocin, LC3II/I and Beclin-1 ( $p < 0.05$ ), and down-regulate the expression of p62, F4/80, NF- $\kappa$ B p65, IL-1 $\beta$ , TNF- $\alpha$  and IL-6 ( $p < 0.05$ ) both in vivo and in vitro, suggesting that Tan-IIA treatment alleviated podocyte injury by promoting autophagy and inhibiting inflammation during DN. The levels of p-PI3K/PI3K, p-Akt/Akt and p-mTOR/mTOR in Tan-IIA group were lower than those in DN group ( $p < 0.05$ ), indicating that Tan-IIA inhibited the PI3K/Akt/mTOR signalling pathway in podocytes, which was a key pathway in regulating both autophagy and inflammation.

**Conclusion:** Tan-IIA prevented podocyte injury in DN by fostering autophagy and inhibiting inflammation, at least in part via inhibition of the PI3K/Akt/mTOR signalling pathway.

**Keywords:** tanshinone IIA, podocyte, diabetic nephropathy, autophagy, inflammation, PI3K/Akt/mTOR signalling pathway

## Introduction

Diabetic nephropathy (DN) is a chronic microvascular complication of diabetes mellitus and the leading cause of end-stage renal disease.<sup>1</sup> Studies have shown that strict blood sugar and blood pressure control as well as blocking renin-angiotensin-aldosterone system and other standard treatment strategies can only delay the progression of DN, but not prevent or reverse it.<sup>2</sup> Therefore, it is essential to explore the pathophysiology of DN and develop effective early treatment methods.

DN is caused by a number of factors, including decreased glomerular filtration rate, the deposition of extracellular matrix, the accumulation of advanced glycation end products, and oxidative stress damage. To some extent, these complex mechanisms harm the glomerular filtration barrier.<sup>3</sup> Podocytes are an important component of the glomerular filtration barrier. Podocytes are highly specialized and terminally differentiated cells with limited mitotic ability.<sup>4</sup> Podocyte dysfunction has been shown to be an important risk factor for glomerular disease and can lead to the development of DN proteinuria.<sup>5</sup>

The basic autophagy activity of podocytes is very high under normal physiological conditions, indicating that the autophagic lysosome system is important in maintaining podocyte homeostasis.<sup>5</sup> Autophagy refers to the formation of autophagosomes by engulfing part of the cytoplasm, organelles, and proteins that need to be degraded. Autophagosomes combine with lysosomes to form autolysosomes, which degrade inclusions, stabilize the intracellular environment, and regenerate organelles.<sup>6</sup> Numerous studies have shown that podocyte autophagy activity is inhibited significantly in DN.<sup>7,8</sup> Inflammation also plays a significant role in the pathogenesis of DN as a downstream pathway of classical pathogenesis, such as glucose metabolism disorder, hemodynamic disorder, and oxidative stress injury.<sup>9</sup>

The mTOR pathway is the classic signal in autophagy studies. Recent studies have revealed that specifically blocking the mTOR pathway promotes autophagy, reducing podocyte damage and renal dysfunction.<sup>10</sup> The PI3K/Akt signalling pathway allows mTOR to participate in autophagy.<sup>11</sup> Furthermore, the PI3K/Akt pathway not only directly induces NF- $\kappa$ B to cause inflammation, but also plays a role in regulating the inflammatory response of macrophages after phosphorylation of Akt to trigger the downstream mTOR expression.<sup>12,13</sup>

*Salvia miltiorrhiza* Bunge, the dry root and rhizome of the herbaceous plant *Salvia miltiorrhiza* Bunge of Lamiaceae family, has been used in traditional Chinese medicine for many centuries as a valuable medicinal herb with antioxidative, antifibrotic, and anti-inflammatory potential.<sup>14</sup> Several studies have suggested that *Salvia miltiorrhiza* Bunge or its components prevent vascular diseases and inflammatory diseases.<sup>15,16</sup> Tanshinone IIA (Tan-IIA), an extract of *Salvia miltiorrhiza* Bunge, is fat soluble. With anti-inflammatory and antioxidant properties, it protects against several diseases, including DN.<sup>17</sup> Tan-IIA can inhibit inflammatory factor expression and release, as well as reduce mononuclear macrophage infiltration in the glomerulus during DN.<sup>18</sup> In addition, recent studies have found that Tan-IIA can induce autophagy in diseases, such as renal ischemia-reperfusion injury, and has the effect of interfering with PI3K/Akt/mTOR and other autophagy-related pathways in cardiovascular diseases and tumours.<sup>19,20</sup> However, the effects of Tan-IIA on podocyte autophagy in DN remains unclear. It is necessary to further explore whether it regulates PI3K/Akt/mTOR pathway to intervene autophagy and inflammation in podocytes.

## Materials and Methods

### Materials and Reagents

Tan-IIA (Molecular Weight: 294.34, content = 99.5%) was isolated from the *Salvia miltiorrhiza* Bunge (The full botanical plant names have been checked with <http://www.worldfloraonline.org>). Tan-IIA was obtained from the National Institutes for Food and Drug Control (Beijing, China, CAS No. 568–72–9), and was dissolved in 0.5% carboxymethyl cellulose solution (Regen Biotechnology Co., Ltd, Beijing, China, CAS No. 9000–11–7) for intragastric administration. Irbesartan was purchased from the Sanofi Pharmaceutical Co., Ltd. (Hangzhou, China).

### Animal Experiment

Eight-week-old male db/db mice and db/m mice were provided by the Jiangsu Jicuiyaokang Biotechnology Co., Ltd (Nanjing, China, License no. SCXK 2018–0008). Without specific pathogens, all mice were kept at room temperature (20–26°C) in a 12 h light/dark cycle and under a constant relative humidity (40–70%). During the experiment, they were allowed to eat and drink freely. All the experiments followed the National Institutes of Health Guide for the Care and Use of Laboratory Animals. The Ethics Committee of Xuzhou Medical University approved this experimental project (202101A103).

According to the conversion ratio of surface area between mice and humans (9.1),<sup>21</sup> the daily dose of Tan-IIA for mice was calculated to be 20 mg/kg, which was taken as the medium dose. Half or twice the median dose, 10 mg/kg and 40 mg/kg were used as the low and high dose groups, respectively.<sup>22</sup> After 1 week, all db/db mice were randomly assigned to one of the five groups: (1) DN group; (2) irbesartan group (IRB group); (3) High-dose tanshinone IIA group (Tan-H group); (4) Medium-dose tanshinone IIA group (Tan-M group); and (5) Low-dose tanshinone IIA group (Tan-L group). The control group consisted of the db/m littermate mice. The db/db mice were treated with Tan-IIA 10 mg/kg/day, 20 mg/kg/day, and 40 mg/kg/day respectively, and irbesartan 20 mg/kg/day by gavage for 12 weeks. An equal volume of 0.5% sodium carboxymethyl cellulose was administered by gavage daily to the DN group and control group.

## Cell Experiment

Murine kidney podocyte cell line MPC5 was provided by Beijing Beina Chuanglian Biotechnology Research Institute (Beijing, China, Cat. No. BNCC342021). Cells were cultured at 37°C in a humidified incubator with 5% CO<sub>2</sub> in RPMI-1640 medium (Servicebio, Wuhan, China, Cat. No. G4530-500ML) containing 5.5 mM D-glucose (GLP BIO, USA, CAS No. 50–99-7), 1% penicillin/streptomycin (Gibco, USA, Cat. No. 15140–122), and 10% foetal bovine serum (Gibco, USA, Cat. No. 10099–141) after resuscitation.<sup>23</sup> Our previous study showed that adding 35 mM D-glucose to the medium for 48 h could cause MPC5 cells damage. The cell viability was increased significantly after intervention with 30 μM Tan-IIA for 48 h. Mannitol was used as an osmotic control in this project. As autophagy inhibitors and activators, 3-MA (5 mM in ultrapure water) and rapamycin (10 μM in dimethyl sulfoxide) were also used.<sup>24</sup> The D-mannitol (CAS No. 69–65-8), 3-MA (CAS No. 5142–23-4), and rapamycin (CAS No. 53123–88-9) were all purchased from Sigma-Aldrich (St. Louis, MO, USA). The cell experiment included six groups: (1) control group (5.5 mM D-glucose); (2) mannitol group (5.5 mM D-glucose + 29.5 mM D-mannitol); (3) HG group (35 mM D-glucose); (4) HG + Tan-IIA group (35 mM D-glucose + 30 μM Tan-IIA); (5) HG + Tan-IIA + rapamycin group (35 mM D-glucose + 30 μM Tan-IIA + 10 μM rapamycin); and (6) HG + Tan-IIA + 3-MA group (35 mM D-glucose + 30 μM Tan-IIA + 5 mM 3-MA).

## Urine, Serum, and Renal Cortex Tissue Collection

All mice were put in separate metabolic cages for 24 h to collect urine after gavage treatment for 12 weeks. The next day, fasting mice were weighed and blood was drawn after anaesthesia. Bilateral kidneys were obtained from the mice after euthanasia. After removal of the renal capsule, the renal cortex was segmented into appropriate sizes. Some were dehydrated and embedded in paraffin after being fixed in 4% paraformaldehyde (Vicmed, Xuzhou, China, Cat. No. VIC357) for 24 h. Then, they were segmented into 4 μm sections for both hematoxylin-eosin (HE) and immunohistochemical (IHC) staining. The other parts were divided into pieces about 2mm, fixed, and examined under a transmission electron microscope. The remaining renal cortex was frozen and stored in freezer tubes at –80°C.

## Biochemical Indicators Measurement

The urinary albumin, urine creatinine, serum creatinine (Scr), blood urea nitrogen (BUN), and blood glucose were examined by the kits, following the manufacturer's instructions. All kits were provided by Nanjing Jiancheng BioEngineering Institute (Nanjing, China).

## Hematoxylin-Eosin Staining

All sections were routinely dewaxed, rehydrated, stained for 5 min with haematoxylin solution, differentiated in hydrochloric acid ethanol for 5s, blued for 30s with blue solution or warm water, and washed by distilled water. After that, they were sequentially submerged for 5 min each in 85% ethanol, 95% ethanol, and eosin stain. Finally, the slides were successively dehydrated in ethanol and xylene. Neutral glue was added to the centre of the slides and covered to prevent air bubbles. All sections were examined using an optical microscope (BX53, Olympus Corporation, Japan).

## Immunohistochemical Assay

The sections were routinely dewaxed and rehydrated. Sections were blocked with 5% H<sub>2</sub>O<sub>2</sub> for 10 min, then blocked by goat serum for 20 min at 37°C, after being treated with the antigen retrieval solution at 95°C for 20 min. Then they were incubated with the primary antibodies F4/80 (Cat. No. 28463-1-AP), LC3 (Cat. No. 14600-1-AP), and p62 (Cat. No. 18420-1-AP) (Proteintech Biotechnology, Wuhan, China) overnight at 4°C, before the secondary antibodies were added for 30 min at 37°C. Hematoxylin staining was carried out for 5 min following a 20-minute DAB solution incubation. The cumulative optical density was calculated using Image-Pro Plus software (Media Cybernetics, USA).

## Observation of the Glomerular Ultrastructure

In order to rinse the fixed renal cortical tissue, 0.1 M phosphate buffer (pH 7.4) was used. Then, the specimen was dehydrated with graded ethanol, soaked in isoamyl acetate, dried, and treated conventionally. The glomerular ultrastructure was examined using a transmission electron microscope (JEM1400PLUS, JEOL Ltd, Japan).

## Western Blotting Analysis

Using a mixture of protease inhibitors, phosphatase inhibitors, and RIPA lysates, proteins were taken out of MPC5 cells and renal cortical tissue. A BCA kit (Beyotime, Shanghai, China, Cat. No. P0010) was used to measure protein concentrations. An 8–15% separation gel and a 5% concentration gel were set up in a glass plate. Total protein was added to the electrophoresis tank after gelation. The protein was separated by electrophoresis and then moved to a polyvinylidene fluoride (PVDF) membrane.<sup>25</sup> The primary antibodies Synaptopodin (Cat. No. 21064-1-AP), Podocin (Cat. No. 20384-1-AP), IL-1 $\beta$  (Cat. No. 16806 -1-AP), LC3 (Cat. No. 14600-1-AP), p62 (Cat. No. 18420-1-AP), Bcln-1 (Cat. No. 11306-1-AP), NF- $\kappa$ B p65 (Cat. No. 10745-1-AP) (Proteintech Biotechnology, Wuhan, China), IL-6 (Cat. No. 12912), TNF- $\alpha$  (Cat. No. 11948), Akt (Cat. No. 4691), p-Akt (Cat. No. 4060) (Cell Signaling Technology, USA), PI3K (Cat. No. AF6241), p-PI3K (Cat. No. AF3241), mTOR (Cat. No. AF6308), p-mTOR (Cat. No. AF3308) (Affinity Biosciences, Wuhan, China), and  $\beta$ -actin (Bioss, Beijing, China, Cat. No. bs-0061R) were used to incubate the PVDF membrane, and then the fluorescence secondary antibody was added. Finally, the optical density of each image was calculated using ImageJ software. Membranes were horizontally cut to probe proteins with different molecular weights.

## Immunofluorescence Detection

4% paraformaldehyde was used to fix the cells for 30 min in each group. The blocking solution, which contained 10% goat serum and 0.3% Triton X-100, was applied and blocked for 30 min. Following that, primary antibodies Synaptopodin (1:200), Podocin (1:100), p62 (1:100), LC3 (1:250), and NF- $\kappa$ B p65 (1:100) were applied to the cells overnight at 4°C. Then secondary antibody conjugated with Alexa Fluor 488 (1:300) was added to incubate for 2 h in the dark. Images were taken under an inverted fluorescence microscope (Olympus IX73, Japan) after the DAPI nuclear staining solution incubated the cells in dark for 5 min.

## Statistical Analysis

Statistical analysis was performed using GraphPad Prism 9.0 (GraphPad Software, USA). The measurement data were expressed as mean  $\pm$  standard deviation (Mean  $\pm$  SD). When the data conformed to the normal distribution and met the homogeneity of variance, one-way ANOVA was used and the pairwise comparison between groups were performed using the Least Significance Difference method, otherwise nonparametric test was used. At *P* values < 0.05, the difference was statistically significant.

## Results

### Tan-IIA Improved Renal Dysfunction in db/db Mice

The Scr, BUN, blood glucose, and urinary albumin/creatinine ratio (ACR) of the mice were detected. [Figure 1A–D](#) demonstrated that the DN group had higher blood glucose, BUN, Scr, and urinary ACR levels than the control group. The urinary ACR and Scr levels were decreased in the Tan-L group, Tan-M group, Tan-H group as well as the irbesartan group in comparison with the DN group. Additionally, compared to the DN group, the BUN level was reduced in the Tan-H group. Blood glucose level was not statistically different among groups of db/db mice.

### Tan-IIA Alleviated Renal Pathological Damage in DN Mice

In the control group, the glomerular structure was intact and renal tubules were properly organized, according to HE staining. In comparison with the control group, the DN group had an increased glomerular volume, partial tubular

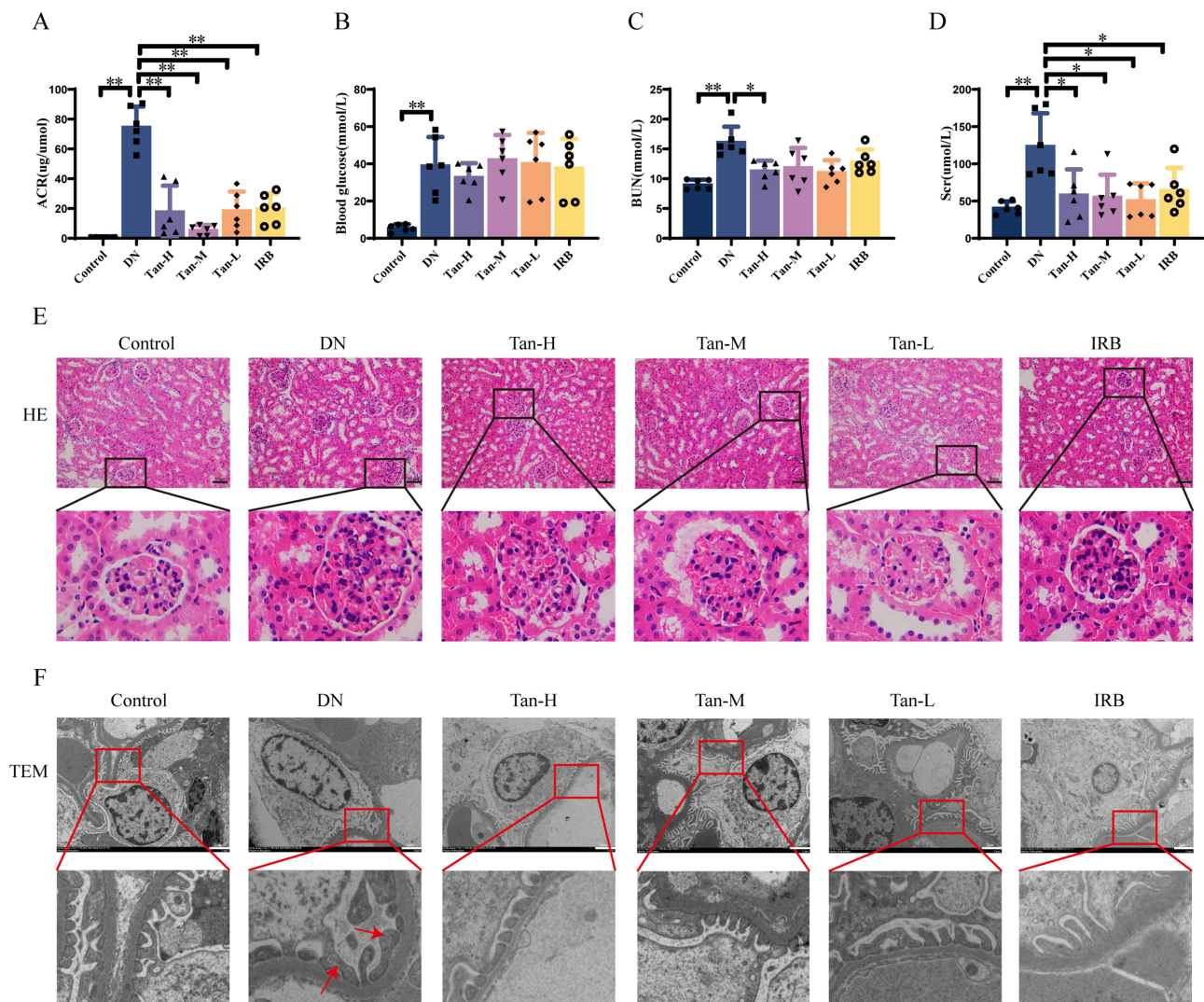


**Figure 1** Effect of Tan-IIA treatment on biochemical parameters and renal histological damage in mice. (A–D) Urinary albumin/creatinine ratio (ACR), blood glucose, blood urea nitrogen (BUN), and serum creatinine (Scr) levels in each group (n=6). (E and F) Renal pathological changes were analyzed by hematoxylin-eosin (scale bar = 50  $\mu$ m) and ultrastructural changes of glomerulus were detected by transmission electron microscopy (scale bar = 2  $\mu$ m). In the DN group, foot process fusion was shown by the red arrow. Data were expressed as mean  $\pm$  SD. Statistical significance was determined by one-way ANOVA. \* $p$  < 0.05, \*\* $p$  < 0.01.

degeneration, and inflammatory cell infiltration. The Tan-L group, Tan-M group, Tan-H group as well as the irbesartan group had lighter lesions in the glomerulus and tubules than those in the DN group (Figure 1E).

## Tan-IIA Prevented Podocyte Injury Under High Glucose Conditions

The morphology and distribution of podocytes, as well as the glomerular basement membrane, were all normal in the control group, with no obvious foot process detachment or fusion, according to the examination of transmission electron microscopy. Thickened glomerular basement membrane, mesangial matrix dilation, and mass fusion or loss of foot processes (foot process fusion was shown by the red arrow) were observed in DN mice compared to the control group. The Tan-L group, Tan-M group, Tan-H group, and the irbesartan group had considerably less changes in glomerular basement membrane thickness and podocyte morphology than the DN group (Figure 1F). Synaptopodin and Podocin, two structural proteins of podocytes, were examined by Western blotting. Synaptopodin and Podocin expression in the DN group was lower than that in the control group. This implied a decrease in the number of normal podocytes in the DN group. The Tan-L group, Tan-M group, Tan-H group, and the irbesartan group all showed higher expression of Synaptopodin and Podocin in comparison with the DN group, indicating that podocyte damage was improved (Figure 2A–C).

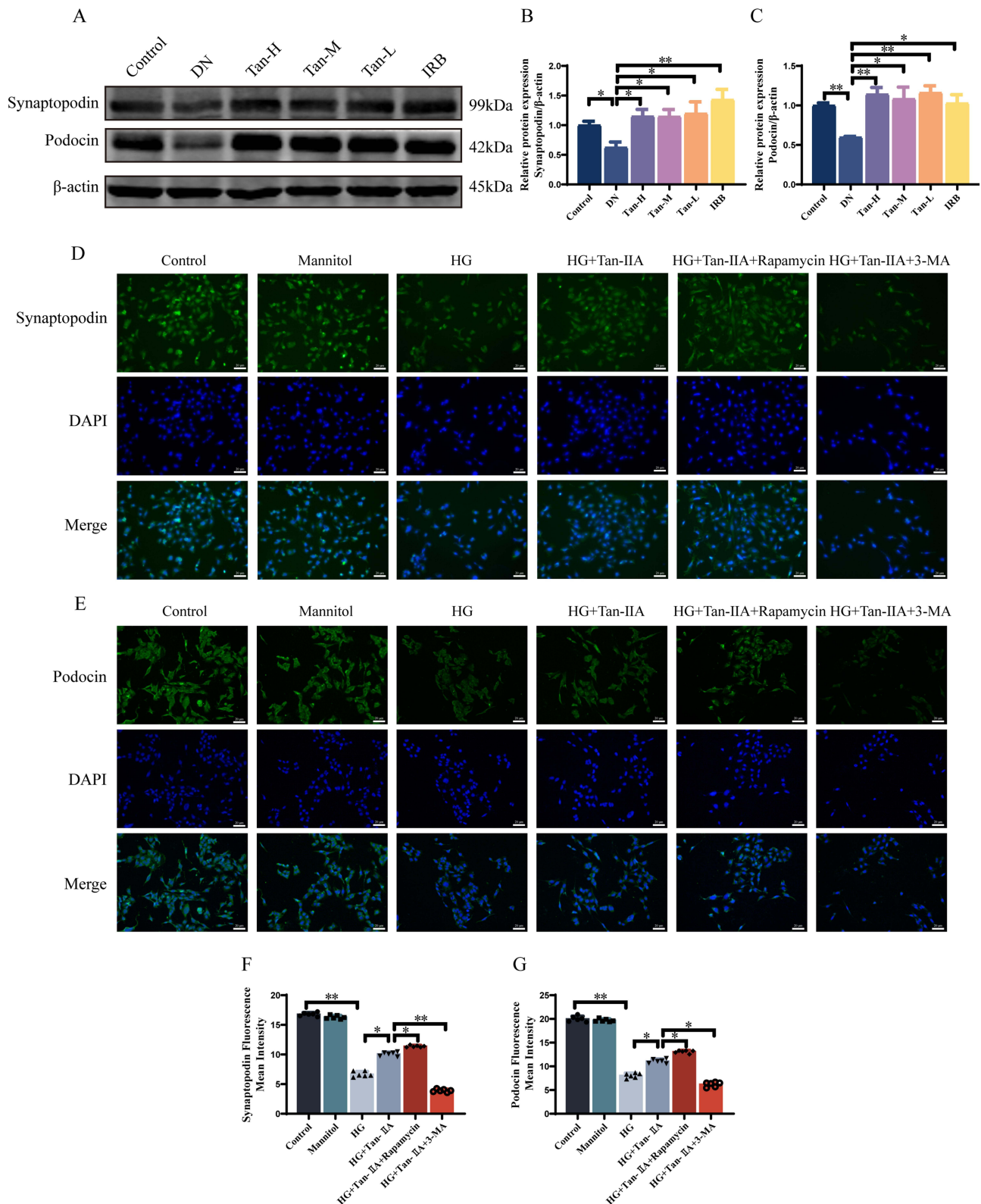


**Figure 2** Effect of Tan-IIA treatment on podocyte injury. **(A)** Protein levels of Synaptopodin and Podocin in renal cortical tissues were detected by Western blotting (n=3). **(B and C)** Protein concentration analysis. **(D and E)** The amount of Synaptopodin and Podocin protein in MPC5 cells was revealed by immunofluorescence staining (scale bar = 20  $\mu$ m, n=6). **(F and G)** Image-J software was used to analyze the immunofluorescence staining results. Data were expressed as mean  $\pm$  SD. Statistical significance was determined by one-way ANOVA. \* $p < 0.05$ , \*\* $p < 0.01$ .

In vitro, immunofluorescence results revealed that the podocyte markers Synaptopodin and Podocin in the HG group were less expressed than in the control group. Compared with the HG group, Tan-IIA increased Synaptopodin and Podocin expression. Tan-IIA's protective role in podocytes was validated by these findings (Figure 2D–G).

## Tan-IIA Fostered Autophagy in Podocytes

Electron microscopy images of the glomerulus in the control group (Figure 3A) showed autophagosomes, which were also seen in the Tan-L group, Tan-M group, Tan-H group, and the irbesartan group (autophagosomes were shown by the red arrow). Fewer autophagosomes were found in the DN group. p62 and LC3 expression in the glomerulus were detected by IHC staining to understand the role of Tan-IIA in autophagy of podocytes (Figure 3B–E). Compared with the control group, the expression of p62 was higher in the DN group, whereas the LC3 expression was lower. In contrast to the DN group, p62 level was considerably decreased in the Tan-L group, Tan-M group, Tan-H group, and the irbesartan group, while LC3 level was increased. The expression of p62, Beclin-1, and LC3 in renal cortical tissues was also tested by Western blotting. The above proteins are critical in autophagy and are frequently employed to assess autophagic flux. LC3II/I and Beclin-1 levels in the DN group were lower than those in the control group, while p62 level was higher, indicating that autophagy was suppressed. The Tan-L group, Tan-M group, and the irbesartan group reduced the level of p62, while the Tan-L group, Tan-M group, Tan-H group, and the irbesartan group increased LC3 II/I and Beclin-1 levels (Figure 3F–I).

The HG group had a higher level of p62 and lower expression of LC3 than the control group. When compared to the HG group, Tan-IIA treatment dramatically upregulated LC3 expression and reduced p62 expression. These were in line with the findings of in vivo experiments. Tan-IIA combined with rapamycin, an autophagy agonist, further enhanced LC3 expression and lowered p62 level compared to Tan-IIA alone in MPC5 cells. After the addition of the autophagy inhibitor 3-MA, the LC3 level fell and the p62 level rose in comparison with the Tan-IIA group (Figure 4). This result also indicated that Tan-IIA could interfere with podocyte autophagy.

## Tan-IIA Inhibited Glomerular Inflammation in DN

Next, how Tan-IIA regulated glomerular inflammation in DN was investigated. The expression of macrophage marker F4/80 in each group was observed by IHC staining (Figure 5A). Inflammatory factors NF- $\kappa$ B p65, IL-1 $\beta$ , TNF- $\alpha$ , and IL-6 were identified by Western blotting (Figure 5B). In comparison with the controls, the F4/80 level was higher in the DN group. In the Tan-L group, Tan-M group, Tan-H group, and the irbesartan group, F4/80 expression was considerably lower than in the DN group (Figure 5C). The DN group had higher expression of these inflammatory factors than the control group. NF- $\kappa$ B p65 and IL-1 $\beta$  levels in the Tan-L group, Tan-M group, Tan-H group, and the irbesartan group were significantly decreased in comparison with the DN group. TNF- $\alpha$  expression was also reduced in the Tan-L group, Tan-H group, and the irbesartan group. IL-6 expression was lower in the Tan-M group, Tan-H group, and the irbesartan group than in the DN group (Figure 5D–H). These results indicated that Tan-IIA inhibited glomerular inflammation in DN, possibly via blocking the NF- $\kappa$ B signalling pathway.

Immunofluorescence staining findings showed that HG promoted the transport of NF- $\kappa$ B p65 into the nucleus in MPC5 cells as compared to the control group (Figure 5I). As opposed to the HG group, Tan-IIA treatment dramatically reduced the transport of NF- $\kappa$ B p65 into the nucleus. Compared with Tan-IIA alone, Tan-IIA combined with rapamycin further reduced the transport of NF- $\kappa$ B p65 into the nucleus. Furthermore, when the autophagy inhibitor 3-MA was added to the Tan-IIA group, the transport of NF- $\kappa$ B p65 into the nucleus was enhanced.

## Tan-IIA Blocked the PI3K/Akt/mTOR Signalling Pathway

An essential signalling pathway that regulates autophagy and inflammation is PI3K/Akt/mTOR. Therefore, studies on the protein expression of this pathway were done both in vivo and in vitro. In vivo, the glomerulus of DN showed activation of the PI3K/Akt/mTOR signalling pathway, as evidenced by the enhanced expression of p-PI3K, p-Akt, and p-mTOR in the DN group when compared with the control group. p-PI3K, p-Akt, and p-mTOR levels were reduced in the Tan-L group, Tan-M group, Tan-H group as well as the irbesartan group compared to the DN group (Figure 6A and C–E). The results were validated by Western blotting in MPC5 cells to further confirm the effects of Tan-IIA on the PI3K/Akt/mTOR signalling pathway during DN. In comparison with the control group, the HG group had increased levels of p-PI3K, p-Akt, and p-mTOR. Comparing Tan-IIA to the HG group, the levels of the aforementioned proteins were drastically decreased. Tan-IIA combined

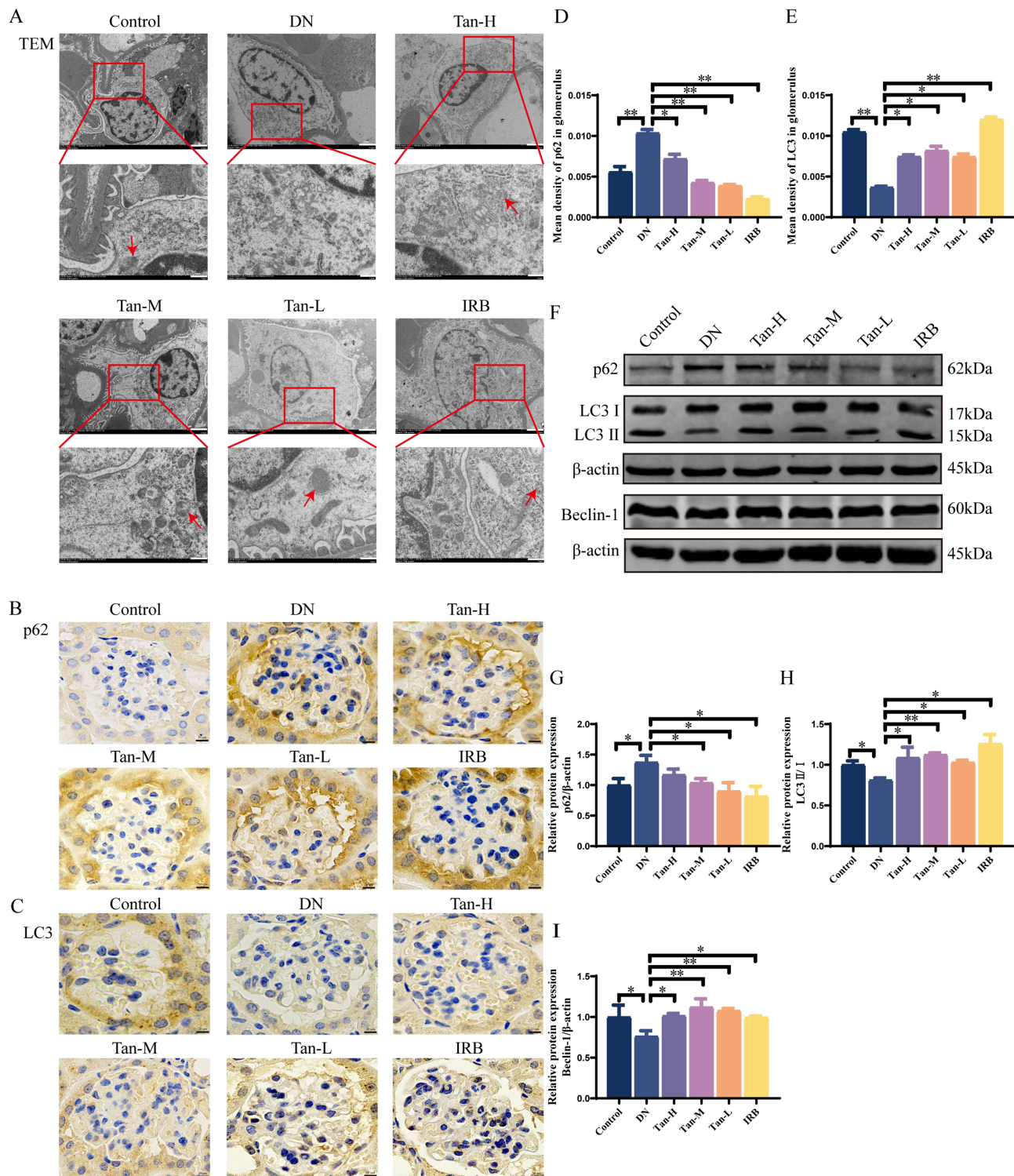


**Figure 3** Effect of Tan-IIA treatment on glomerular autophagy. **(A)** Autophagosomes in glomerulus were observed (red arrow) and photographed by transmission electron microscopy (scale bar = 2 μm). **(B and C)** p62 and LC3 expression in glomerulus were detected by immunohistochemistry (scale bar = 20 μm, n=3). **(D and E)** Image-Pro Plus software was used to analyze the mean density of p62 and LC3 in glomerulus. **(F)** Western blotting was used to detect p62, LC3II/I and Beclin-1 protein levels in renal cortical tissues (n=3). **(G–I)** Protein concentration analysis. Data were expressed as mean ± SD. Statistical significance was determined by one-way ANOVA. \* $p < 0.05$ , \*\* $p < 0.01$ .

with rapamycin further decreased these proteins expression compared with Tan-IIA alone. After adding the autophagy inhibitor 3-MA, these proteins levels rose in comparison with the Tan-IIA group (Figure 6B and F–H). These results showed that, in podocytes under high glucose conditions, Tan-IIA inhibited the PI3K/Akt/mTOR signalling pathway.



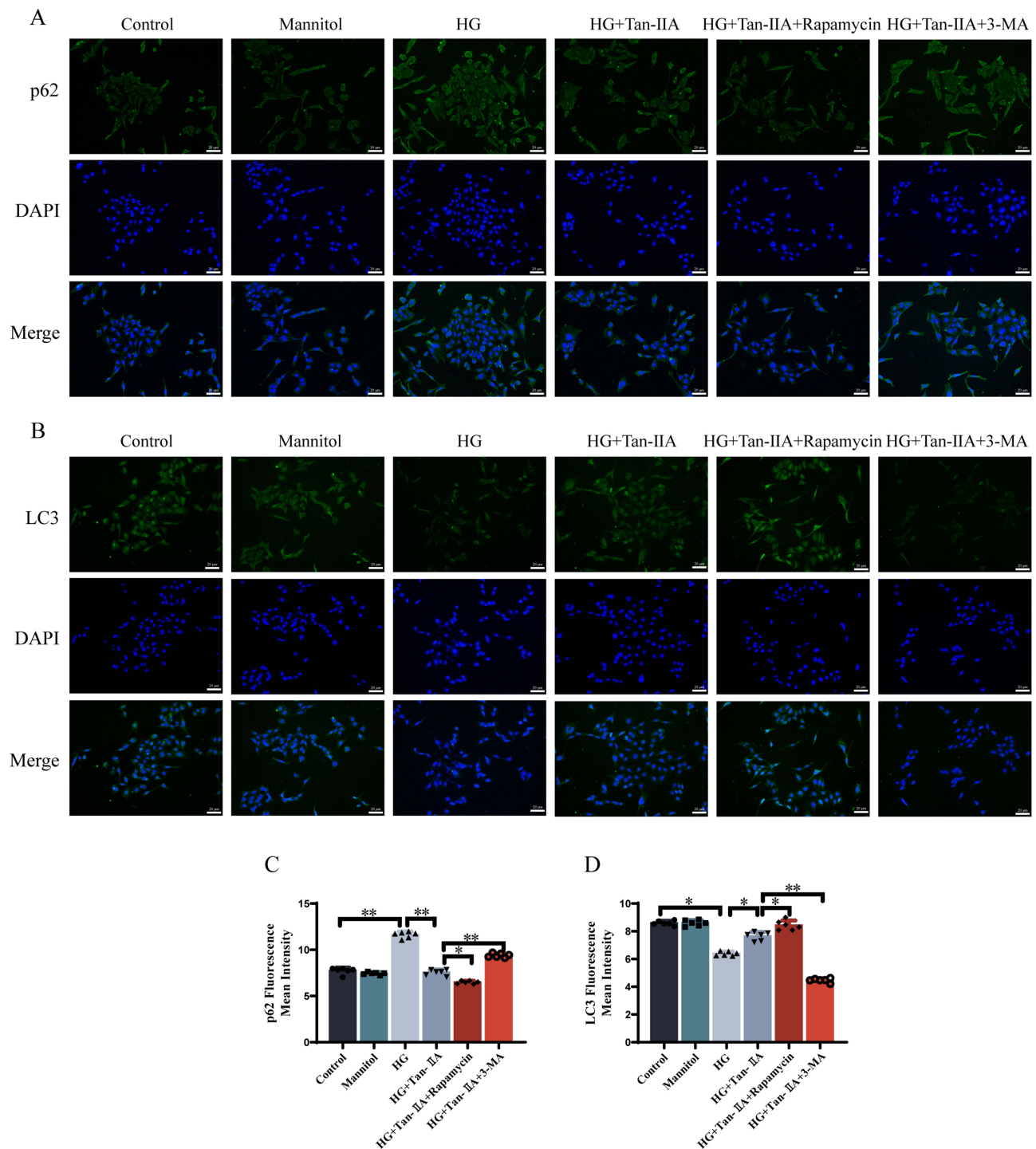


**Figure 4** Effect of Tan-IIA treatment on MPC5 cells autophagy. **(A and B)** The amount of p62 and LC3 protein in MPC5 cells was revealed by immunofluorescence staining (scale bar = 20  $\mu$ m, n=6). **(C and D)** Image-J software was used to analyze the immunofluorescence staining results. Data were expressed as mean  $\pm$  SD. Statistical significance was determined by one-way ANOVA. \* $p < 0.05$ , \*\* $p < 0.01$ .

## Discussion

Mesangial expansion, basement membrane thickening, and podocyte injury are the most common pathological manifestations of DN.<sup>26</sup> There is compelling evidence that early podocyte loss promotes DN progression.<sup>27,28</sup> Therefore, the focus of this research was on the damage to glomerular podocytes in DN and investigating how to protect podocytes and improve DN.

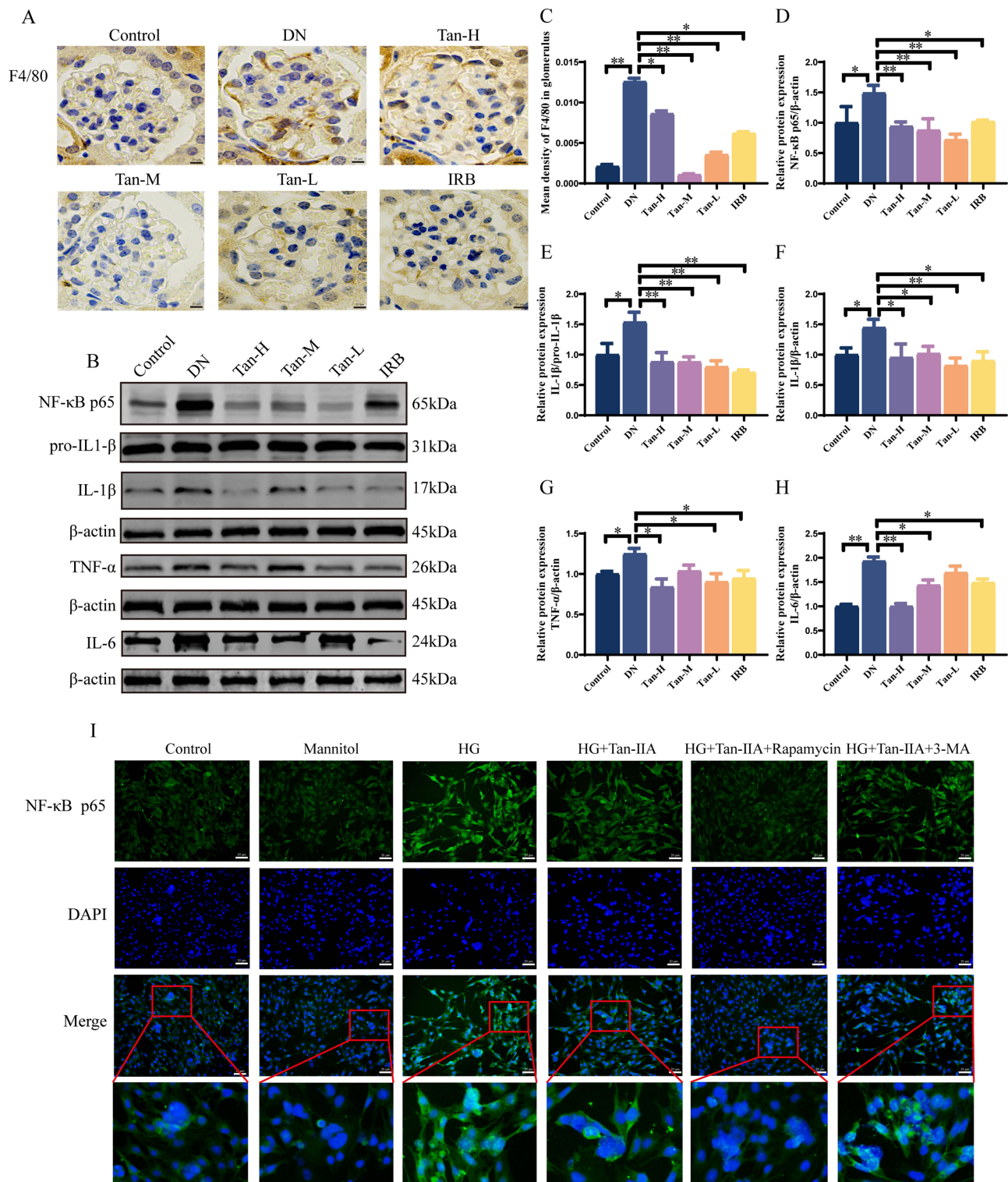


**Figure 5** Effect of Tan-IIA treatment on inflammatory response in vivo and in vitro. **(A)** F4/80 expression in glomerulus were detected by immunohistochemistry (scale bar = 20  $\mu$ m, n=3). **(B)** Western blotting was used to detect NF- $\kappa$ B p65, IL-1 $\beta$ , TNF- $\alpha$ , and IL-6 protein levels in renal cortical tissues (n=3). **(C)** Image-Pro Plus software was used to analyze the mean density of F4/80 in glomerulus. **(D–H)** Protein concentration analysis. **(I)** Immunofluorescence staining was used to observe the nuclear translocation of NF- $\kappa$ B p65 in MPC5 cells among six groups (scale bar = 20  $\mu$ m). Data were expressed as mean  $\pm$  SD. Statistical significance was determined by one-way ANOVA. \* $p$  < 0.05, \*\* $p$  < 0.01.

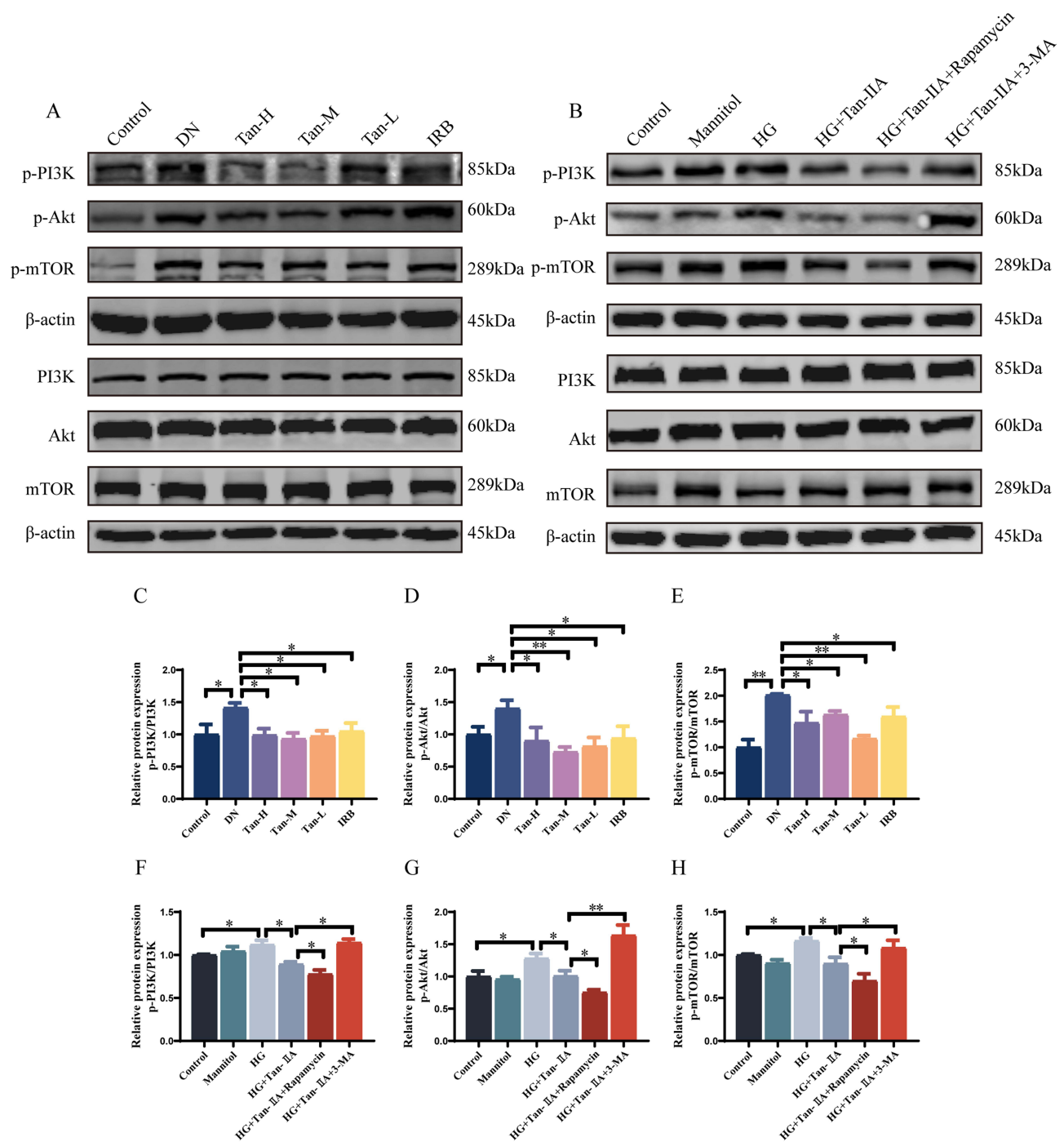


**Figure 6** Effect of Tan-IIA treatment on PI3K/Akt/mTOR Signalling Pathway. **(A)** Protein levels of p-PI3K, PI3K, p-Akt, Akt, p-mTOR, and mTOR in renal cortical tissues were detected by Western blotting (n=3). **(B)** Protein expression of p-PI3K, PI3K, p-Akt, Akt, p-mTOR, and mTOR in MPC5 cells were detected by Western blotting (n=3). **(C–H)** Protein concentration analysis. Data were expressed as mean  $\pm$  SD. Statistical significance was determined by one-way ANOVA. \* $p < 0.05$ , \*\* $p < 0.01$ .

Traditional Chinese medicines have been used for centuries to treat diabetes and diabetic complications and have gained popularity in recent years due to their remarkable clinical efficacy.<sup>16</sup> *Salvia miltiorrhiza* Bunge has definite effects and benefits to prevent and treat diabetic vascular disease in early. Tan-IIA is the main diterpene compound found in *Salvia miltiorrhiza* Bunge, which can reduce vascular intimal hyperplasia, improve tissue blood perfusion and renal microcirculation, promote anticoagulation, and reduce damage to the kidneys.<sup>29</sup> The role of Tan-IIA on podocyte autophagy and inflammation during DN were mainly observed in this work.

Irbesartan, an angiotensin II receptor blocker, is a representative medication for the clinical treatment of DN and has been shown in clinical trials to lower proteinuria significantly in patients.<sup>30,31</sup> Studies have suggested the potential effects of irbesartan against doxorubicin-induced renal dysfunction by inducing autophagy, anti-inflammatory, and anti-apoptotic effects that may be, in part, mediated by AMPK, PI3K/Akt, and mTOR signalling pathways.<sup>32</sup> As a result, for the pharmacological research of Tan-IIA, irbesartan was chosen as a positive control drug. In this study, irbesartan promoted autophagy, inhibited inflammation, and suppressed the PI3K/Akt/mTOR signalling pathway. The difference between the irbesartan group and Tan-IIA groups were indistinguishable.

The C57BLKS leptin receptor knockout mice called db/db mice were used in the current research. This mouse line has characteristics similar to those of the Jackson Laboratory mouse line: significant increases in body weight beginning at 4 weeks, hyperglycaemia at 8 weeks, insulinemia at 8 weeks, and hyperlipidaemia along with the early onset of renal dysfunction at 12 weeks.<sup>33</sup> As a result, investigations on DN have frequently employed this mouse line as a model. In the DN group, the urinary ACR as well as the blood glucose, BUN, and Scr levels were increased. After 12 weeks of gavage treatment, the Tan-IIA group had lower urinary ACR and Scr levels than the DN group. Tan-IIA could improve pathological changes, such as increase of glomerular volume, expansion of mesangial matrix, and damage of podocyte ultrastructure in the DN group, according to HE staining and transmission electron microscopy observation. These results suggested that Tan-IIA could protect glomerular podocytes and alleviate the damage of renal structure and function during DN.

Podocyte hypertrophy, epithelial-mesenchymal transition, podocyte detachment, and podocyte apoptosis in DN affect the morphology and number of podocytes.<sup>34</sup> Synaptopodin and Podocin, the structural proteins in podocytes, were detected by Western blotting in order to assess podocyte injury. Lower levels of Synaptopodin and Podocin suggested that podocytes were damaged and the levels of normal podocytes were decreased. The findings revealed that the Synaptopodin and Podocin expression in the DN group were significantly reduced than those in the control group, whereas Tan-IIA significantly increased these levels. Tan-IIA's ability to lessen podocyte damage in vitro with MPC5 cells was also validated.

Studies conducted in vivo and in vitro showed that podocyte autophagy is reduced, and its integrity is disrupted, during DN. It has also been demonstrated that increasing autophagy decreases podocyte damage.<sup>35,36</sup> Atg12-ATG5 and Atg16L1 promote the binding of LC3 to PE and recruit LC3-II to the autophagosomal membrane in order for the autophagosome to extend. Thus, LC3-II is regarded as a crucial marker for assessing autophagosomes.<sup>37</sup> Beclin-1 is the first autophagy gene to be found in mammalian cells, and it can positively regulate autophagy.<sup>38</sup> Another common autophagy marker, p62, binds directly to LC3 and GABARAP family of proteins through a short LC3 interaction area. During this process, autophagy degrades the p62 protein, which serves as a marker for studying autophagy flux.<sup>39</sup> In this study, it was found that Tan-IIA increased LC3II/I and Beclin-1 levels while decreased p62 level of the glomerulus in db/db mice. This implied that Tan-IIA promoted glomerular autophagy during DN.

Tan-IIA's effects on podocyte autophagy were further tested using autophagy agonists and inhibitors in vitro. 3-MA is an autophagy inhibitor that prevents cells from forming autophagosomes.<sup>40</sup> Rapamycin, on the other hand, is an autophagy activator capable of simulating cell starvation.<sup>41</sup> In MPC5 cells, incubation with rapamycin enhanced Tan-IIA's boosting impact on autophagy in high glucose conditions, but incubation with 3-MA inhibited Tan-IIA's promoting effect. These results provided support for the hypothesis that Tan-IIA promoted autophagy and shielded podocytes from damage.

Chronic inflammation is well known to play an important role in the development of DN. Macrophages are one of the major inflammatory/immune cells that infiltrate the kidneys in diabetic conditions, causing a proinflammatory environment in almost all renal cells, leading to extracellular matrix accumulation, fibrosis, cell dysfunction, and eventually proteinuria.<sup>42</sup> The NF- $\kappa$ B pathway stimulates a series of inflammatory processes, resulting in an increased extracellular matrix and glomerular podocyte injury, and ultimately aggravates renal dysfunction by up-regulating the expression of inflammatory factors, such as NF- $\kappa$ B p65, F4/80, IL-1 $\beta$ , IL-6, and TNF- $\alpha$ .<sup>43</sup> Podocyte injury under inflammatory conditions has been shown to play a critical role in the development of DN.<sup>44</sup> Higher levels of F4/80, NF- $\kappa$ B p65, IL-1 $\beta$ , TNF- $\alpha$ , and IL-6 were found in the renal cortex of the DN group in this work. When compared to the DN group, Tan-IIA considerably decreased the level of these inflammatory factors, indicating that inflammation was inhibited.

Podocyte injury occurs when the balance between mTOR activity and autophagy activity is disrupted.<sup>45</sup> Both in vivo and in vitro researches showed that the p-mTOR increased in the DN group. Tan-IIA could decrease the p-mTOR level. The activity of the mTOR pathway is primarily regulated by the PI3K/Akt pathway, and the PI3K/Akt/mTOR signalling pathway is involved in signal transduction and autophagosome formation during podocyte autophagy.<sup>46</sup> High glucose can activate PI3K/Akt/mTOR and cause

podocyte injury. As a result, regulating the PI3K/Akt/mTOR signalling pathway reduces podocyte injury.<sup>47</sup> Here, studies conducted in vivo and in vitro showed that p-PI3K and p-Akt levels were dramatically increase in the DN group. Tan-IIA inhibited these proteins expression. Tan IIA promoted autophagy, at least in part, via inhibiting the PI3K/Akt pathway, which regulates the activity of the mTOR pathway. The PI3K/Akt pathway can directly activate the NF- $\kappa$ B pathway, leading to inflammation.<sup>48</sup> Comparing Tan-IIA to the HG group, the amount of NF- $\kappa$ B p65 that transported into the nucleus was significantly reduced in vitro. Tan-IIA combined with rapamycin further reduced the transport of NF- $\kappa$ B p65 into the nucleus compared to the Tan-IIA group. In addition, compared to Tan-IIA, the transport of NF- $\kappa$ B p65 into the nucleus was increased after the addition of autophagy inhibitor 3-MA. Thus, it was proposed that Tan-IIA regulated the PI3K/Akt/mTOR signalling pathway not only to promote autophagy, but also to inhibit inflammation. This might be one of the ways in which Tan-IIA preserves glomerular podocytes to improve DN.

Studies conducted in vivo and in vitro have supported Tan-IIA's ability to protect glomerular podocytes in DN. However, there remain some flaws. Tan-IIA was administered to mice in the current study at doses of 10 mg/kg/d, 20 mg/kg/d, and 40 mg/kg/d, respectively. In the results, all three doses of Tan-IIA showed protective effect on glomerular podocytes with no significant dose-dependence, which was likely due to the small sample size. In subsequent studies, we will use a single effective dose of Tan-IIA in accordance with the three *Rs* (replacement, refinement, and reduction) concept in ethical animal research.

## Conclusion

This study confirmed that Tan-IIA can preserve glomerular podocytes and alleviate renal damage in DN. Tan-IIA regulated the PI3K/Akt/mTOR signalling pathway to promote autophagy and inhibit inflammation, thereby alleviating podocyte injury (Figure 7). This might be the reason for the renal protective effect of Tan-IIA. The findings point to Tan-IIA as a suitable option to prevent and treat DN, making it potentially worthy of further investigation.

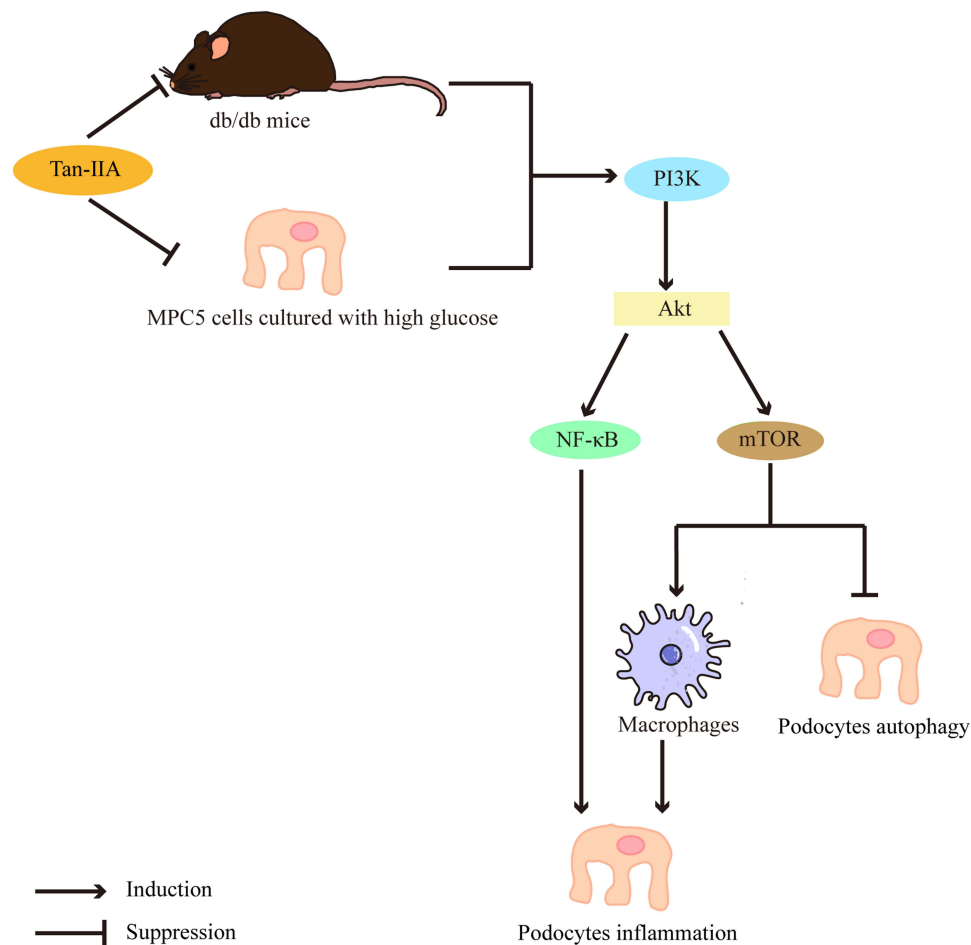


**Figure 7** Mechanism of Tan-IIA administration on podocyte injury in diabetic nephropathy.

## Abbreviations

ACR, Urinary albumin/creatinine ratio; Akt, Serine/threonine-protein kinase B; Atg, Autophagy-related genes; BUN, Blood urea nitrogen; DN, Diabetic nephropathy; HG, High glucose; IL-6, Interleukin 6; IL-1 $\beta$ , Interleukin 1 $\beta$ ; LC3, Microtubule-associated protein light chain 3; MPC5, Mouse podocyte clone-5; mTOR, Mammalian target of rapamycin; NF- $\kappa$ B, Nuclear factor-kappa B; PI3K, Phosphatidylinositide 3-kinases; p62, Ubiquitin-binding protein p62; Scr, Serum creatinine; TNF- $\alpha$ , Tumor necrosis factor alpha; 3-MA, 3-Methyladenine.

## Data Sharing Statement

The data will be available from the corresponding author on request.

## Author Contributions

All authors made a significant contribution to the work reported, whether that is in the conception, study design, execution, acquisition of data, analysis and interpretation, or in all these areas; took part in drafting, revising or critically reviewing the article; gave final approval of the version to be published; have agreed on the journal to which the article has been submitted; and agree to be accountable for all aspects of the work.

## Funding

Grants from National Natural Science Foundation of China (NO. 81804059) and Natural Science Foundation of Jiangsu Province (BK20180996) helped to fund this research.

## Disclosure

The authors report no conflicts of interest in this work.

## References

1. Sago MK, Gnudi L. Diabetic nephropathy: an overview. *Methods Mol Biol.* 2020;2067:3–7. doi:10.1007/978-1-4939-9841-8\_1
2. Samsu N. Diabetic nephropathy: challenges in pathogenesis, diagnosis, and treatment. *Biomed Res Int.* 2021;2021:1497449. doi:10.1155/2021/1497449
3. Podgórski P, Konieczny A, Lis Ł, Witkiewicz W, Hruby Z. Glomerular podocytes in diabetic renal disease. *Adv Clin Exp Med.* 2019;28(12):1711–1715. doi:10.17219/acem/104534
4. Sugita E, Hayashi K, Hishikawa A, Itoh H. Epigenetic alterations in podocytes in diabetic nephropathy. *Front Pharmacol.* 2021;12:759299. doi:10.3389/fphar.2021.759299
5. Lin Q, Banu K, Ni Z, Leventhal JS, Menon MC. Podocyte autophagy in homeostasis and disease. *J Clin Med.* 2021;10(6). doi:10.3390/jcm10061184
6. Cao W, Li J, Yang K, Cao D. An overview of autophagy: mechanism, regulation and research progress. *Bull Cancer.* 2021;108(3):304–322. doi:10.1016/j.bulcan.2020.11.004
7. Dong W, Jia C, Li J, et al. Fisetin attenuates diabetic nephropathy-induced podocyte injury by inhibiting NLRP3 inflammasome. *Front Pharmacol.* 2022;13:783706. doi:10.3389/fphar.2022.783706
8. Su PP, Liu DW, Zhou SJ, Chen H, Wu XM, Liu ZS. Down-regulation of Risa improves podocyte injury by enhancing autophagy in diabetic nephropathy. *Mil Med Res.* 2022;9(1):23. doi:10.1186/s40779-022-00385-0
9. Wu K, Peng R, Mu Q, et al. Rack1 regulates pro-inflammatory cytokines by NF- $\kappa$ B in diabetic nephropathy. *Open Med.* 2022;17(1):978–990. doi:10.1515/med-2022-0487
10. Ou Y, Zhang W, Chen S, Deng H. Baicalin improves podocyte injury in rats with diabetic nephropathy by inhibiting PI3K/Akt/mTOR signaling pathway. *Open Med.* 2021;16(1):1286–1298. doi:10.1515/med-2021-0335
11. Kma L, Baruah TJ. The interplay of ROS and the PI3K/Akt pathway in autophagy regulation. *Biotechnol Appl Biochem.* 2022;69(1):248–264. doi:10.1002/bab.2104
12. Vergadi E, Ieronymaki E, Lyroni K, Vaporidi K, Tsatsanis C. Akt signaling pathway in macrophage activation and M1/M2 polarization. *J Immunol.* 2017;198(3):1006–1014. doi:10.4049/jimmunol.1601515
13. Xing Y, Wei H, Xiao X, et al. Methylated Vnn1 at promoter regions induces asthma occurrence via the PI3K/Akt/NF $\kappa$ B-mediated inflammation in IUGR mice. *Biol Open.* 2020;9(4). doi:10.1242/bio.049106
14. Lu TC, Wu YH, Chen WY, Hung YC. Targeting oxidative stress and endothelial dysfunction using tanshinone IIA for the treatment of tissue inflammation and fibrosis. *Oxid Med Cell Longev.* 2022;2022:2811789. doi:10.1155/2022/2811789
15. Kim SK, Jung KH, Lee BC. Protective effect of tanshinone IIA on the early stage of experimental diabetic nephropathy. *Biol Pharm Bull.* 2009;32(2):220–224. doi:10.1248/bpb.32.220
16. Liu XJ, Hu XK, Yang H, et al. A review of traditional Chinese medicine on treatment of diabetic nephropathy and the involved mechanisms. *Am J Chin Med.* 2022:1–41. doi:10.1142/s0192415x22500744

17. Li W, Sargsyan D, Wu R, et al. DNA methylome and transcriptome alterations in high glucose-induced diabetic nephropathy cellular model and identification of novel targets for treatment by tanshinone IIA. *Chem Res Toxicol*. 2019;32(10):1977–1988. doi:10.1021/acs.chemrestox.9b00117
18. Li Y, Deng X, Zhuang W, et al. Tanshinone IIA down-regulates -transforming growth factor beta 1 to relieve renal tubular epithelial cell inflammation and pyroptosis caused by high glucose. *Bioengineered*. 2022;13(5):12224–12236. doi:10.1080/21655979.2022.2074619
19. Ding L, Ding L, Wang S, et al. Tanshinone IIA affects autophagy and apoptosis of glioma cells by inhibiting phosphatidylinositol 3-Kinase/Akt/Mammalian Target of Rapamycin Signaling Pathway. *Pharmacology*. 2017;99(3–4):188–195. doi:10.1159/000452340
20. Pan Y, Qian JX, Lu SQ, et al. Protective effects of tanshinone IIA sodium sulfonate on ischemia-reperfusion-induced myocardial injury in rats. *Iran J Basic Med Sci*. 2017;20(3):308–315. doi:10.22038/ijbms.2017.8361
21. Han W, Zhang L, Yu LJ, Wang JQ. Effect of local delivery of vancomycin and tobramycin on bone regeneration. *Orthop Surg*. 2021;13(5):1654–1661. doi:10.1111/os.13020
22. Wang W, Long H, Huang W, et al. Bu-Shen-Huo-Xue decoction ameliorates diabetic nephropathy by inhibiting Rac1/PAK1/p38MAPK signaling pathway in high-fat diet/streptozotocin-induced diabetic mice. *Front Pharmacol*. 2020;11:587663. doi:10.3389/fphar.2020.587663
23. Yang F, Qu Q, Zhao C, et al. Paecilomyces cicadae-fermented Radix astragali activates podocyte autophagy by attenuating PI3K/AKT/mTOR pathways to protect against diabetic nephropathy in mice. *Biomed Pharmacother*. 2020;129:110479. doi:10.1016/j.biopha.2020.110479
24. Li X, Ma A, Liu K. Geniposide alleviates lipopolysaccharide-caused apoptosis of murine kidney podocytes by activating Ras/Raf/MEK/ERK-mediated cell autophagy. *Artif Cells Nanomed Biotechnol*. 2019;47(1):1524–1532. doi:10.1080/21691401.2019.1601630
25. Xuan C, Xi YM, Zhang YD, Tao CH, Zhang LY, Cao WF. Yiqi jiedu huayu decoction alleviates renal injury in rats with diabetic nephropathy by promoting autophagy. *Front Pharmacol*. 2021;12:624404. doi:10.3389/fphar.2021.624404
26. Nie P, Lou Y, Bai X, et al. Influence of zinc levels and Nrf2 expression in the clinical and pathological changes in patients with diabetic nephropathy. *Nutr Diabetes*. 2022;12(1):37. doi:10.1038/s41387-022-00212-4
27. Jaimes EA, Zhou MS, Siddiqui M, et al. Nicotine, smoking, podocytes, and diabetic nephropathy. *Am J Physiol Renal Physiol*. 2021;320(3):F442–F453. doi:10.1152/ajprenal.00194.2020
28. Lu CC, Wang GH, Lu J, et al. Role of Podocyte Injury in Glomerulosclerosis. *Adv Exp Med Biol*. 2019;1165:195–232. doi:10.1007/978-981-13-8871-2\_10
29. Chen X, Wu R, Kong Y, et al. Tanshinone IIA attenuates renal damage in STZ-induced diabetic rats via inhibiting oxidative stress and inflammation. *Oncotarget*. 2017;8(19):31915–31922. doi:10.18632/oncotarget.16651
30. Liu J, Zhang J, Hou MH, Du WX. Clinical efficacy of linagliptin combined with irbesartan in patients with diabetic nephropathy. *Pak J Med Sci*. 2022;38(1):52–56. doi:10.12669/pjms.38.1.4417
31. Abdel-Wahab AF, Bmagous GA, Al-Harizy RM, et al. Renal protective effect of SGLT2 inhibitor dapagliflozin alone and in combination with irbesartan in a rat model of diabetic nephropathy. *Biomed Pharmacother*. 2018;103:59–66. doi:10.1016/j.biopha.2018.03.176
32. Mohamed EA, Ahmed HI, Zaky HS. Protective effect of irbesartan against doxorubicin-induced nephrotoxicity in rats: implication of AMPK, PI3K/Akt, and mTOR signaling pathways. *Can J Physiol Pharmacol*. 2018;96(12):1209–1217. doi:10.1139/cjpp-2018-0259
33. Li HQ, Liu N, Zheng ZY, Teng HL, Pei J. Clopidogrel delays and can reverse diabetic nephropathy pathogenesis in type 2 diabetic db/db mice. *World J Diabetes*. 2022;13(8):600–612. doi:10.4239/wjdv13.i8.600
34. Dai H, Liu Q, Liu B. Research progress on mechanism of podocyte depletion in diabetic nephropathy. *J Diabetes Res*. 2017;2017:2615286. doi:10.1155/2017/2615286
35. Li XZ, Jiang H, Xu L, et al. Sarsasapogenin restores podocyte autophagy in diabetic nephropathy by targeting GSK3 $\beta$  signaling pathway. *Biochem Pharmacol*. 2021;192:114675. doi:10.1016/j.bcp.2021.114675
36. Yuan S, Liang X, He W, Liang M, Jin J, He Q. ATF4-dependent heme-oxygenase-1 attenuates diabetic nephropathy by inducing autophagy and inhibiting apoptosis in podocyte. *Ren Fail*. 2021;43(1):968–979. doi:10.1080/0886022x.2021.1936040
37. Parzych KR, Klionsky DJ. An overview of autophagy: morphology, mechanism, and regulation. *Antioxid Redox Signal*. 2014;20(3):460–473. doi:10.1089/ars.2013.5371
38. Jiang P, Mizushima N. LC3- and p62-based biochemical methods for the analysis of autophagy progression in mammalian cells. *Methods*. 2015;75:13–18. doi:10.1016/j.ymeth.2014.11.021
39. Bjørkøy G, Lamark T, Brech A, et al. p62/SQSTM1 forms protein aggregates degraded by autophagy and has a protective effect on huntingtin-induced cell death. *J Cell Biol*. 2005;171(4):603–614. doi:10.1083/jcb.200507002
40. Shi Y, Tao M, Ma X, et al. Delayed treatment with an autophagy inhibitor 3-MA alleviates the progression of hyperuricemic nephropathy. *Cell Death Dis*. 2020;11(6):467. doi:10.1038/s41419-020-2673-z
41. Lu H, Yang HL, Zhou WJ, et al. Rapamycin prevents spontaneous abortion by triggering decidual stromal cell autophagy-mediated NK cell residence. *Autophagy*. 2021;17(9):2511–2527. doi:10.1080/15548627.2020.1833515
42. Wu M, Han W, Song S, et al. NLRP3 deficiency ameliorates renal inflammation and fibrosis in diabetic mice. *Mol Cell Endocrinol*. 2018;478:115–125. doi:10.1016/j.mce.2018.08.002
43. Hu N, Wang C, Dai X, et al. Phillygenin inhibits LPS-induced activation and inflammation of LX2 cells by TLR4/MyD88/NF- $\kappa$ B signaling pathway. *J Ethnopharmacol*. 2020;248:112361. doi:10.1016/j.jep.2019.112361
44. Cheng Q, Pan J, Zhou ZL, et al. Caspase-11/4 and gasdermin D-mediated pyroptosis contributes to podocyte injury in mouse diabetic nephropathy. *Acta Pharmacol Sin*. 2021;42(6):954–963. doi:10.1038/s41401-020-00525-z
45. Song S, Qiu D, Shi Y, et al. Thioredoxin-interacting protein deficiency alleviates phenotypic alterations of podocytes via inhibition of mTOR activation in diabetic nephropathy. *J Cell Physiol*. 2019;234(9):16485–16502. doi:10.1002/jcp.28317
46. Chen J, Yuan S, Zhou J, et al. Danshen injection induces autophagy in podocytes to alleviate nephrotic syndrome via the PI3K/AKT/mTOR pathway. *Phytomedicine*. 2022;107:154477. doi:10.1016/j.phymed.2022.154477
47. Zhang Y, Wang Y, Luo M, et al. Elabela protects against podocyte injury in mice with streptozocin-induced diabetes by associating with the PI3K/Akt/mTOR pathway. *Peptides*. 2019;114:29–37. doi:10.1016/j.peptides.2019.04.005
48. El-Hanboshi SM, Helmy MW, Abd-Alhaseeb MM. Catalpol synergistically potentiates the anti-tumour effects of regorafenib against hepatocellular carcinoma via dual inhibition of PI3K/Akt/mTOR/NF- $\kappa$ B and VEGF/VEGFR2 signaling pathways. *Mol Biol Rep*. 2021;48(11):7233–7242. doi:10.1007/s11033-021-06715-0

Diabetes, Metabolic Syndrome and Obesity

Dovepress

### Publish your work in this journal

Diabetes, Metabolic Syndrome and Obesity is an international, peer-reviewed open-access journal committed to the rapid publication of the latest laboratory and clinical findings in the fields of diabetes, metabolic syndrome and obesity research. Original research, review, case reports, hypothesis formation, expert opinion and commentaries are all considered for publication. The manuscript management system is completely online and includes a very quick and fair peer-review system, which is all easy to use. Visit <http://www.dovepress.com/testimonials.php> to read real quotes from published authors.

Submit your manuscript here: <https://www.dovepress.com/diabetes-metabolic-syndrome-and-obesity-journal>